JOURNAL OF EXPERIMENTAL AND THEORETICAL PHYSICS, 2024, VOL. 165, No. 1, pp. 106–118

## ORDER, DISORDER, AND PHASE TRANSITION IN CONDENSED MEDIA

# SPIN-ORBIT COUPLING MEDIATED SIZE EFFECTS IN MAGNETORESISTANCE OF Ta NANOLAYERS

© 2024 V. V. Ustinov[a, b*], L. I. Naumova[a, b], R. S. Zavornitsyn[a, b], I. A. Yasyulevich[a], I. K. Maksimova[a], T. P. Krinitsina[a], A. Y. Pavlova[a], V. V. Proglyado[a], M. A. Milyaev[a, b]

[a] *Mikheev Institute of Metal Physics, Ural Branch, Russian Academy of Sciences, Ekaterinburg, 620137 Russia*

[b] *Yeltsin Ural Federal University, Institute of Natural Sciences and Mathematics, Ekaterinburg, 620002 Russia*

* *e-mail: ustinov@imp.uran.ru*

Received 26.07.2023
Revised 26.07.2023
Accepted 24.08.2023

**Abstract**. The theory of size effects in the magnetoresistance of thin films of normal metals due to spin-orbit interaction, which takes into account the surface scattering of conduction electrons with spin reversal, has been constructed. Experimental studies of structural and galvanomagnetic properties of β-tantalum thin films of different thicknesses prepared by magnetron sputtering have been carried out. Based on the analysis of experimental data within the framework of the constructed theory, estimates of the spin diffusion length, spin relaxation time, and spin Hall angle for β-tantalum thin films were made.

**Keywords**: spin-orbit interaction, spin current, spin Hall effect, inverse spin Hall effect, Hanle magnetoresistance, spin diffusion length

**DOI:** 10.31857/S00444510240102e3

## 1. INTRODUCTION

One of the possible mechanisms for generating a spin current without using magnetic materials or a magnetic field is the spin Hall effect. The cause of this effect is the spin-orbit coupling [1–9]. The spin-orbit coupling leads to the fact that the flow of an electric current in a non- magnetic ("normal") metal in the absence of an external magnetic field causes the appearance of transverse pure spin current, which is not accompanied by the transfer of an electric charge [3, 10-15]. In the case of the reverse spin Hall effect, the flow of a spin current in a normal metal causes the occurrence of a transverse electric current. These effects are most noticeable in metals with a strong spin-orbit coupling, such as Pt, Ta, W. If such metals are adjacent to layers of magnetic materials as part of a planar nanostructure, then during electric current flows in the nanostructure the change in the magnetic state of the layers caused by the transfer of the spin moment is possible [9, 16-21]. The study of the relationship of spin and charge currents in normal metals with strong spin-orbit coupling, as well as the processes of spin moment transfer in nanostructures containing metals with various types of magnetic ordering, is the subject of the newest branch of spintronics, called spinorbitronics [16-19, 22].

To create spinorbitronics devices, it is extremely important to study the relationship between spin and charge currents in normal metals. In 2007. Dyakonov theoretically showed [23] that in two-dimensional normal metals with strong spin-orbit coupling, the connection of spin and charge currents can be detected using galvanomagnetic experiments. The flowing electric current due to the spin-orbit coupling causes a purely spin current, which leads to the accumulation of nonequilibrium spin density near the edges of the two-dimensional sample. The accumulated spin density diffuses into the depths of the metal, which causes a pure spin current flowing from the faces of the sample. The external magnetic field leads to the suppression of the nonequilibrium spin density, as a result of which electrical resistance increases and reaches the value of the electrical resistance of the material, in which the presence of spin-orbit coupling can be neglected. This type of magnetoresistance, which arises due to the manifestation of a combination of the direct and inverse spin Hall effect, as well as the Hanle effect (the effect of damping of nonequilibrium spin density during

diffusion under conditions of simultaneous precession in a magnetic field), was named by Dyakonov as magnetoresistance due to edge spin accumulation.

This theory has been confirmed in experiments with thin films of normal metals with strong spin-orbit coupling [24–26]. The authors have shown that the external magnetic field applied along the direction of the electric current causes an increase in the electrical resistance of the film. The longitudinal magnetoresistance of a thin metal film with a strong spin-orbit coupling, arising from the suppression of nonequilibrium spin density near the film surfaces, was named by the authors Hanle magnetoresistance by analogy with the well-known magneto-optics effect.

In the work carried out to date on the study of Hanle magnetoresistance, the question of the role of conductivity electron scattering with spin flip on the film surfaces has not been investigated. However, it can be expected that it is the surface scattering with a spin flip that is a factor significantly affecting the suppression of spin accumulation near the surface due to the spin-orbit coupling. In this paper, a theory of dimensional effects due to spin-orbit coupling in the magnetoresistance of thin films of normal metals is constructed, taking into account the surface scattering of electrons with a spin flip. Within the framework of the constructed theory, the analysis of the results of an experimental study of the Hanle magnetoresistance of β-tantalum thin films was carried out.

## 2. THE THEORY OF DIMENSIONAL EFFECTS IN MAGNETORESISTANCE, DUE TO THE SPIN-ORBIT COUPLING

To describe the electron spin transport in a metal with a strong spin-orbit coupling, we use the equations for the density of conduction electrons $N$, spin density $\mathbf{S}$, electron flux density $\mathbf{I}$ and spin current density $\boldsymbol{J}$, formulated in [27, 28]. In these equations, the electron flux density $\mathbf{I}$ is a vector quantity, whereas the density of the spin current $\boldsymbol{J}$ is a second-rank tensor.

Let $\mathbf{E}$ and $\mathbf{B}$ be the electric and magnetic fields acting in the metal, with respect to which we assume that they are homogeneous in space and independent of time. Below, we will limit ourselves to considering the case when the vectors $\mathbf{E}$ and $\mathbf{B}$ are collinear and parallel to the X axis lying in the plane of the film occupying the region $-L / 2 \le z \le +L / 2$, where $L$ is the thickness of the film. In the considered geometry, when currents $\mathbf{I}$ and $\boldsymbol{J}$ flow, the system remains electrically neutral and then $N \equiv N_0$, where $N_0$ is the equilibrium value of the electron density.

Let's denote the relaxation time of the electron pulse in the process of their orbital motion as a $\tau_O$. The relaxation time of the spin of the conduction electrons is denoted as $\tau_S$. To characterize the intensity of the processes of "skew" scattering of conduction electrons due to the presence of spin-orbit coupling, we introduce, following the work [27, 28], the parameter $\tau_{SO}$, which determines the frequency of skew scattering processes $1 / |\tau_{SO}|$. Parameter $\xi = \tau_O / \tau_{SO}$ characterizes the relative intensity of the skew scattering velocity of conduction electrons and can be of any sign, whereas its magnitude is $|\xi| \ll 1$. The parameters of $\tau_O$ and $\tau_S$ characterize the relaxation of the momentum and spin of the electron in the film and may, generally speaking, depend on the thickness of the film $L$.

When describing the electron flow and spin flow, we consider the $\Omega\tau_O \ll 1$ and $\Omega_C\tau_O \ll 1$, where $\Omega = \gamma B$ — precession frequency, $\Omega_C = |e| B / m_e c$ — cyclotron frequency, $\gamma = 2\mu / \hbar$ — gyromagnetic ratio, $\mu = g\mu_B/2$ — magnetic moment of the electron, whose Lande factor is g, $\mu_B$ — Bohr magneton, $m_e$ — effective electron mass, $e$ — electron charge. As a result, the system of equations [27, 28] for vector $\mathbf{I}$ and tensor $\boldsymbol{J}$ takes the form

$$\mathbf{I} = \frac{\sigma_0}{e}\mathbf{E} - \xi\boldsymbol{\epsilon}\cdot\cdot\boldsymbol{J}, \tag{1}$$

$$\boldsymbol{J} = \frac{\sigma_0}{N_0 e}\mathbf{E}\otimes\mathbf{S}_0 - D_0\frac{\partial}{\partial r}\otimes\delta\mathbf{S} - \xi\boldsymbol{\epsilon}\cdot\mathbf{I}, \tag{2}$$

$$\frac{\partial}{\partial\mathbf{r}}\cdot\boldsymbol{J} + \gamma\left[\delta\mathbf{S}\times\mathbf{B}\right] + \frac{1}{\tau_S}\delta\mathbf{S} = 0. \tag{3}$$

Here $\sigma_0 = N_0 e^2\tau_O / m_e$ is the specific conductivity of the Degenerate electron gas in the absence of spin-orbit coupling, $D_0 = v_F^2\tau_O/3$ is the corresponding $\sigma_0$ coefficient of electron diffusion, $v_F$ is the Fermi velocity. The value $\delta\mathbf{S} = \mathbf{S} - \mathbf{S}_0$ is the deviation of the spin density $\mathbf{S}$ from its locally equilibrium value $\mathbf{S}_0 = -\chi\mathbf{B} / \mu$, where $\chi$ is the susceptibility of the Pauli electron gas. The terms «⊗», «·» and «· ·» are used to denote mathematical operations of the tensor, scalar and double scalar product of vectors and tensors, respectively, the symbol $\boldsymbol{\epsilon}$ denotes an absolutely antisymmetric unit tensor of rank 3.

Equation (2) clearly describes a phenomenon called the spin Hall effect: the flow of conduction electrons $\mathbf{I}$, appearing in the last term of the right side of equation (2), induces spin current $\boldsymbol{J}$ by a spin-orbit coupling. Accordingly, equation (1) describes the inverse spin Hall effect: the spin current $\boldsymbol{J}$, in the presence of spin-orbit coupling, induces an electric current $\mathbf{I}$. In the literature devoted to the description of the Hall spin effect, the term spin Hall angle is often used. The spin Hall angle, denoted as $\Theta_{SH}$, is associated with the parameter introduced

by $\xi$ relation $\xi = \mathrm{tg}\Theta_{SH}$. Since it is always $|\Theta_{SH}| \ll 1$, the parameter is $\xi \simeq \Theta_{SH}$.

The solution of the system of equations (1), (2) relative to currents $\mathbf{I}$ and $\boldsymbol{J}$ can be written in the form

$$\mathbf{I} = \frac{\sigma}{e}\mathbf{E} - \xi D\left[\frac{\partial}{\partial \mathbf{r}} \times \delta\mathbf{S}\right], \tag{4}$$

$$\boldsymbol{J} = -\frac{\chi\sigma}{e\mu N_0}\mathbf{E} \otimes \mathbf{B} - D\frac{\partial}{\partial \mathbf{r}} \otimes \delta\mathbf{S} - \xi\frac{\sigma}{e}\boldsymbol{\epsilon} \cdot \mathbf{E}, \tag{5}$$

where $\sigma = \sigma_0 / \left(1 + 2\xi^2\right)$ and $D = D_0 / \left(1 + 2\xi^2\right)$ are the conductivity and diffusion coefficient of the unlimited metal renormalized by the spin-orbit coupling. In obtaining expression (5) for $\boldsymbol{J}$, we neglected the difference between the tensor $\boldsymbol{\epsilon} \cdot \boldsymbol{\epsilon} \cdot \cdot \boldsymbol{J}$ from $\boldsymbol{\epsilon} \cdot \cdot \boldsymbol{\epsilon} \cdot \boldsymbol{J}$, which is insignificant for the purposes of this work.

In the considered configuration of the fields $\mathbf{E}$ and $\mathbf{B}$ relative to the film surface, both the flux of conduction electrons $\mathbf{I}$ and the spin current $\boldsymbol{J}$ can depend on only one spatial coordinate $z$. This allows you to write the vector $\mathbf{I}(z)$ in the form $\mathbf{I}(z) = I_x(z)\mathbf{e}_x$, where $\mathbf{e}_x$ is a unit vector specifying the direction of the $X$ axis, and the only nonzero component of the flux density $I_x(z)$ is determined by equation

$$I_x(z) = \frac{\sigma}{e}E + \xi D\frac{\partial}{\partial z}\delta S_y. \tag{6}$$

It clearly follows from expression (6) that the accumulation of the spin moment of electrons close to the film surfaces caused by the spin-orbit coupling, leading to the dependence of the nonequilibrium spin density $\delta S_y$ on the $z$ coordinate, has as a direct consequence a dependence of the density of the electric current flowing in the film $j(z) = eI_x(z)$ on the $z$ coordinate as well.

In order to make the picture of the flow of the spin current $\boldsymbol{J}$ more visual, we introduce into consideration, following the work [27], the vectors $\mathbf{P}_i$ of polarization of spin currents flowing in the directions $i = x, y, z$, which are given by the unit vectors $\mathbf{e}_i$. By definition, $\mathbf{P}_i = \mathbf{e}_i \cdot \boldsymbol{J}$. Setting three vectors $\mathbf{P}_i$ is completely equivalent to specifying the tensor $\boldsymbol{J}$. In the coordinate system we have chosen from the expression (5) we get

$$\mathbf{P}_x = -\frac{\chi\sigma}{e\mu N_0}EB\mathbf{e}_x, \tag{7}$$

$$\mathbf{P}_y = -\xi\frac{\sigma}{e}E\mathbf{e}_z, \tag{8}$$

$$\mathbf{P}_z = -D\frac{\partial}{\partial z}\delta\mathbf{S} + \xi\frac{\sigma}{e}E\mathbf{e}_y. \tag{9}$$

It follows from expressions (7)–(9) that the vectors $\mathbf{P}_x$ and $\mathbf{P}_y$, which define the polarization of spin currents flowing in the $X$ and $Y$ directions, do not change their shape and direction with a change in the $z$ coordinate. On the contrary, the polarization vector $\mathbf{P}_z$ of the spin current flowing along the $Z$ direction depends on the coordinate $z$ in the most significant way due to the dependence of the nonequilibrium spin density $\delta\mathbf{S}$. Using the vector $\mathbf{P}_z$ equation (3) can be written as follows:

$$\frac{\partial}{\partial z}\mathbf{P}_z + \gamma\left[\delta\mathbf{S} \times \mathbf{B}\right] + \frac{1}{\tau_S}\delta\mathbf{S} = 0. \tag{10}$$

To find the nonequilibrium density $\delta\mathbf{S}(z)$ from equations (9), (10) it is necessary to set boundary conditions connecting the vectors $\mathbf{P}_z(z)$ and $\delta\mathbf{S}(z)$ at the boundaries of the film $z = \pm L / 2$. A detailed derivation of such boundary conditions is presented in [29, 30]. To characterize the spin scattering of conduction electrons at the film boundaries, we introduce a phenomenological parameter $\varepsilon$, which makes sense of the probability of electron scattering with a spin flip when an electron is reflected from the surface of the film. Then the required boundary conditions can be written in the form

$$\mathbf{P}_z\left(\pm L / 2\right) = \pm\frac{\varepsilon}{1-\varepsilon}\frac{v_F}{2}\delta\mathbf{S}\left(\pm L / 2\right). \tag{11}$$

The solution of the equations (9), (10) with boundary conditions (11) can be written as follows

$$\delta S_x = 0, \quad \delta S_y = \mathrm{Re}\delta S, \quad \delta S_z = -\mathrm{Im}\delta S, \tag{12}$$

where

$$\delta S = \xi\frac{\sigma\tau_S E}{eL_S}\frac{\mathrm{sh}\zeta\kappa}{\kappa\mathrm{ch}\lambda\kappa + \psi\mathrm{sh}\lambda\kappa}. \tag{13}$$

When writing expression (13) for $\delta S$ we introduced dimensionless variables $\zeta = z / L_S$, $\beta = \gamma\tau_S B$ and $\kappa = \sqrt{1 + i\beta}$, $\mathrm{Re}\kappa > 0$, as well as parameters $\lambda = L / 2L_S$ and $\psi = \left(\tau_S v_F / 2L_S\right)\varepsilon / \left(1 - \varepsilon\right)$, in which $L_S = \sqrt{\tau_S D}$ is the spin-diffusion length calculated taking into account the spin-orbit coupling.

The formulas (6), (12), (13) show that the spin-orbit coupling leads to an increase in the electric current density near the boundaries of the film compared with the value of the current density in its depth. Integrating the expression for $j$ over $z$ from $-L / 2$ to $+L / 2$, we find the total electric current flowing in the film, which allows us to write the following expression for the specific electrical resistance $\rho_L(B)$ of a film of thickness $L$ in a magnetic field $B$:

$$\rho_L(B) = \rho\left(1 + \frac{\xi^2}{\lambda}\mathrm{Re}\frac{1}{\kappa c\mathrm{th}\lambda\kappa + \psi}\right)^{-1}. \quad (14)$$

Here $\rho = \sigma^{-1}$ is the specific electrical resistivity of the film material, calculated taking into account the spin-orbit coupling of electrons, but without taking into account the surface spin accumulation.

In the absence of a magnetic field , the dimensional effect in the electrical resistance of thin metal layers due to spin-orbit coupling will be described by the value $\rho_L(B=0) \equiv \rho_L$. The expression for $\rho_L$ assuming the smallness of the parameter $\xi^2 \ll 1$ takes the form

$$\rho_L = \left(1 - \frac{\xi^2}{1+\psi\mathrm{th}\lambda}\frac{\mathrm{th}\lambda}{\lambda}\right)\rho. \quad (15)$$

It follows from expression (15) that the scattering of conduction electrons with a spin flip on the surface of the film, described by the parameter $\psi$, leads to a decrease in the size-dependent of the electrical resistance of the film $\rho_L$. This decrease is described by the multiplier $\xi^2/(1+\psi\mathrm{th}\lambda)$ in the right part of expression (15). If condition $\psi \ll 1$, is fulfilled, then the effect of spin-flip scattering on the surface can be neglected.

We introduce into consideration the relative Hanle magnetoresistance $\mathcal{R}_L$ by the formula

$$\mathcal{R}_L(B) = \frac{\rho_L(B) - \rho_L(B=0)}{\rho_L(B=0)}. \quad (16)$$

Due to the fulfillment of the condition $\xi^2 \ll 1$ of (14)–(16) for the Hanle magnetoresistance, we obtain

$$\mathcal{R}_L(B) = \frac{\xi^2}{1+\psi\mathrm{th}\lambda}\frac{\mathrm{th}\lambda}{\lambda}\times \times\left[1 - \mathrm{Re}\left(\frac{\mathrm{th}\lambda\kappa}{\kappa\mathrm{th}\lambda}\frac{1+\psi\mathrm{th}\lambda}{1+\psi\mathrm{th}\lambda\kappa/\kappa}\right)\right]. \quad (17)$$

Defined by the expression (17) relative magnetoresistance $\mathcal{R}_L(B)$ is a positively defined monotonically increasing limited function of the field $B$. With an increase in the magnetic field at values B significantly exceeding the value $B_S = 1/\gamma\tau_S$, the value $\mathcal{R}_L(B)$ reaches its maximum possible value $\mathcal{R}_L^{(max)} \equiv \mathcal{R}_L(B \gg B_S)$. It follows from (17) that

$$\mathcal{R}_L^{(max)} = \xi_L^2\frac{\mathrm{th}\lambda}{\lambda}, \quad (18)$$

where

$$\xi_L = \frac{\xi}{\sqrt{1+\psi\mathrm{th}\lambda}}. \quad (19)$$

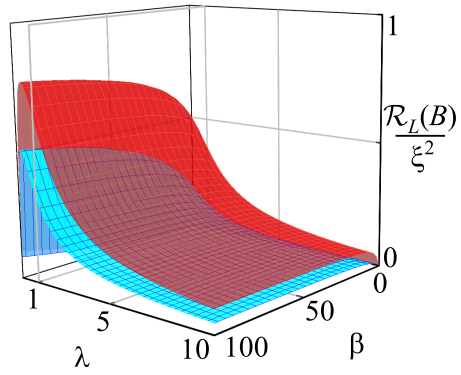


**Fig. 1.** Behavior of $\mathcal{R}_L(B)$ depending on the value $\lambda = L/2L_S$ and $\beta = \gamma\tau_S B$ in the absence of electron scattering on a surface with a spin flip, $\psi = 0$ (red surface), and in the presence of surface scattering with a spin flip, $\psi = 1$ (blue surface)

Magnetoresistance $\mathcal{R}_L^{(max)}$ is a function of thickness $L$ and parametrically depends on the probability of surface scattering with spin flip ε. Dependence $\mathcal{R}_L^{(max)}$ on the thickness is given by the function $\mathrm{th}\lambda/\lambda$ , varying from one to zero with an increase of $\lambda = L/2L_S$, whereas the value of $\mathcal{R}_L^{(max)}$ is determined by the value of the newly introduced parameter $\xi_L$. The parameter $\xi_L$, proportional to ξ and dependent on ε, makes sense of the effective spin Hall angle.

The scattering of electrons on a surface with a spin flip reduces the value of $|\xi_L|$ and thus the magnitude of the magnetoresistance $\mathcal{R}_L^{(max)}$. For any values of the probability ε of scattering on a surface with a spin flip $|\xi_L| \le |\xi|$. If the condition $\psi \ll 1$, is fulfilled, then the effect of surface scattering with a spin flip on the magnetoresistance $\mathcal{R}_L^{(max)}$ can be ignored. Condition $\psi \ll 1$ can be represented as $\varepsilon \ll \sqrt{\tau_O/\tau_S}$.

Fig. 1 shows the behavior of $\mathcal{R}_L(B)$ as a function of the variables β and λ at two different values of the parameter $\psi$.

Fig. 1 shows that for all values of β and λ, the surface scattering of electrons with a spin flip leads to a decrease in the Hanle magnetoresistance. The main contribution to the change of $\mathcal{R}_L(B)$ under the action of surface scattering with a spin flip comes from a decrease in the value of $|\xi_L|$ compared with $|\xi|$.

## 3. EXPERIMENTAL TECHNIQUES

β-tantalum films with a thickness of $L$ = 3, 4, 5, 6.5, 8, 9.5, 11, 14, 30, 57 nm were obtained by the magnetron sputtering method at a power of 100 W on glass substrates. The base pressure of the residual gases in the deposition chamber was $5\cdot10^{-7}$ Pa. The pressure of the argon working gas during deposition Ta was 0.1 Pa.

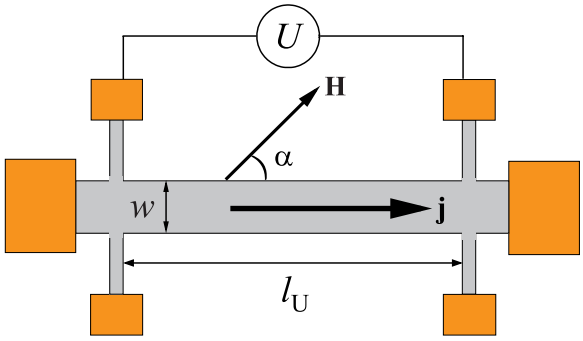


**Fig. 2.** Schematic representation of a micro-object designed for measuring electrical resistance by the four-contact method

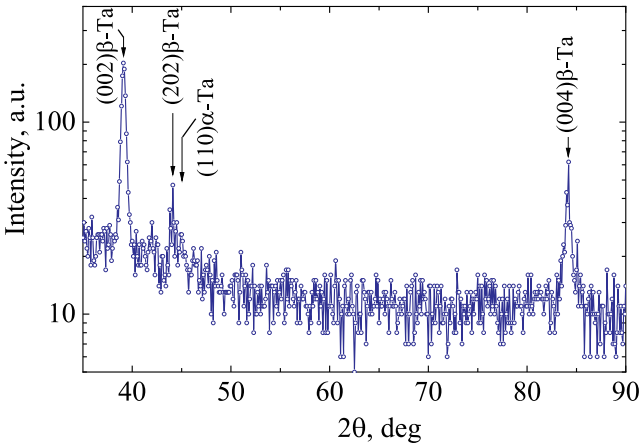


**Fig. 3.** X-ray diffraction pattern of a 57 nm thick tantalum film

Using optical photolithography, micro- objects in the form of Hall bridges were formed from tantalum films (Fig. 2). The width of the microstrips $w$ was 200 microns, the length was 2700 microns, and the distance $l_U$ between potential contacts was 2200 microns. The copper contact pads are formed using the "lift-off" procedure. The electrical resistance of micro-objects was measured in the temperature range 93 ÷ 343K at an installation based on an electric magnet, a pumping cryostat and a temperature controller using a four-contact method. The experimental installation makes it possible to vary the angle α between the direction of the current **j** flowing along the microstrip and the direction of the magnetic field **H** applied in the plane of the film.

The magnetic field when measuring the electrical resistance of the Hall bridges varied within ±20 kOe. The values of the electric current flowing along the Ta microstrips of various thicknesses were not more than 1 mA in order to avoid heating the sample during measurement. The current density did not exceed $1.9 \cdot 10^8$ A/m$^2$.

The microstructure was studied using transmission electron microscopy and X-ray diffraction in Ka Co radiation. The atomic force microscopy method was used to study the surface of thin films.

## 4. STUDY OF THE MICROSTRUCTURE AND SURFACES OF TANTALUM FILMS

Thin Ta films usually have two structure phases: α-Ta with a volume-centered cubic (VCC) structure and β-Ta with a tetragonal crystal lattice [31] and an order of magnitude higher electrical resistivity [32]. Due to the relatively large value of the spin Hall angle, it is β-Ta that represents an interest for creating nanostructures, the magnetic state of which can be changed using an electric current.

We used magnetron sputtering modes in which the β-phase prevails in the Ta layer [33]. Figure 3 shows an X- ray diffraction pattern obtained from a 57 nm thick Ta film. Reflexes from the (002) and (004) planes are visible of the tetragonal structure of β-tantalum and another weak peak that can relate to planes (202), β-Ta or (110), α-Ta.

The appearance of multiple peaks from the planes (002) and the absence of other reflexes of the tetragonal structure is probably a consequence of the texture of {002} in the Ta film.

The results of the transmission electron microscopy study are shown in Fig. 4.

On the electron diffraction pattern obtained from a 57 nm thick Ta film (Fig. 4a), all the observed Debye rings correspond to families of planes of the tetragonal structure of β-tantalum. In Fig. 4 b a dark-field image obtained in a reflex corresponding to a family of planes is shown, {421} or {222}. Sequential dark-field images were obtained by incrementally shifting the masking aperture by a small distance along the Debye ring. The images showed grains sequentially located next to each other. Many neighboring grains are very poorly oriented relative to each other. In the light-field image (Fig. 4c), individual crystals are visible with contrast in the form of dark and light parallel stripes, which is typical for twin defects of the structure. The grain size varies between 6.5 ÷ 25 nm.

The electron diffraction pattern obtained for the Ta film with a thickness of 8 nm (Fig. 4 d) shows diffused Debye rings characteristic of a pseudo-amorphous misoriented fine-crystalline phase. Due to the large width of the rings, the interplanar distances cannot be calculated accurately. According to the position of the middle, the Debye rings belong to the tetragonal structure of β-Ta. Individual point reflexes from larger crystallites are visible on the rings. In the dark-field image (Fig. 4 e) in reflex, {421}, {222} individual crystallites

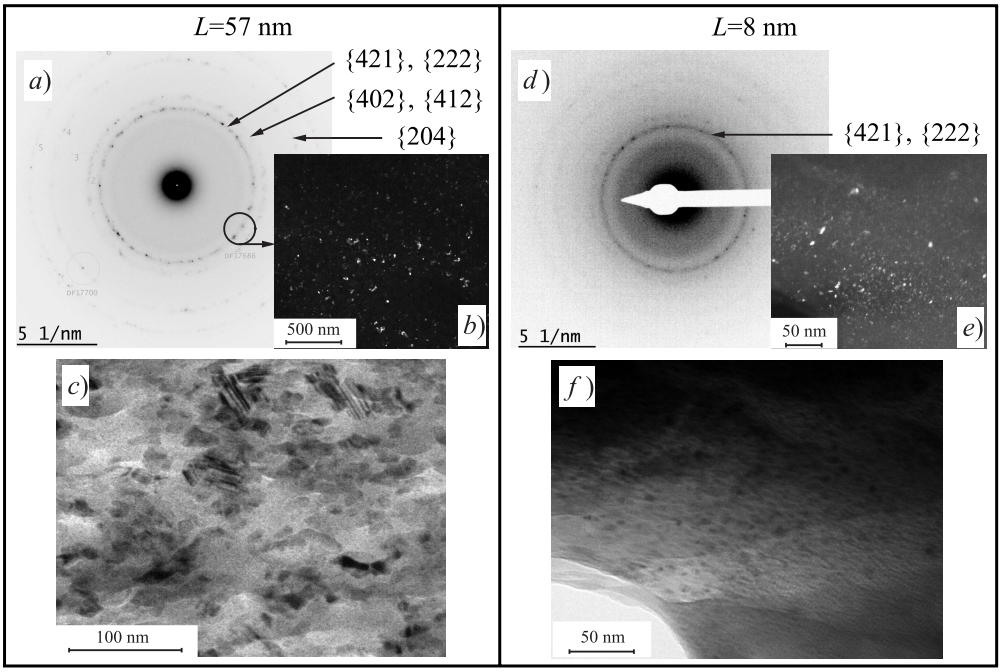


**Fig. 4.** Electron diffraction patterns (a, d), dark-field (b, e) and light-field (c, f) images obtained for tantalum films with a thickness of 57 nm and 8 nm. The dark-field images were obtained in the reflex {421}, {222}

of the appropriate orientation are visible. The grain size varies between 0.6 ÷ 2 nm.

Thus, a pseudo amorphous beta-Ta phase is formed in tantalum films with a thickness of 8 nm. When the film thickness increases to 57 nm, larger crystallites appear and the grain size increases tenfold. The inter-grain boundaries are small-angle. There are packaging defects in the form of double borders.

Fig. 5. Surface images (a, c) and surface profiles (b, d) of 30 and 8 nm thick Ta films

Characteristic images of the β-Ta film surface with thicknesses of 8 and 30 nm obtained by atomic force microscopy are shown in Fig. 5.

With a film thickness of $L = 30$ nm, the average grain size is 17 nm, which is consistent with the crystallite size estimate performed using electron microscopy. When the film thickness is $L = 8$ nm in the surface image, clusters ranging in size from 5 to 25 nm are visible, combining grains whose size is beyond the device's resolution.

Fig. 5 b and Fig. 5 d show the surface profiles of β-Ta films with a thickness of 30 and 8 nm. It can be seen that the surface roughness increases as the film thickness increases.

Fig. 6 shows the dependence of the roughness parameter of the root mean square (RMS) on the thickness of the β-Ta film.

The RMS value was estimated at the site in the size of $1 \times 1$ mm$^2$, averaging was carried out by 3 to 5 measurements in different sections of the sample. Films with a thickness of $L \leqslant 8$ nm have very low roughness. As the film thickness increases, the value of RMS increases significantly.

## 5. GALVANOMAGNETIC PROPERTIES TANTALUM NANOLAYERS

Fig. 7 shows the dependence of the specific electrical resistance of β-Ta films on the thickness at $T = 93$ K in the absence of an external magnetic field.

At $L > 30$ nm, the electrical resistivity practically does not depend on the thickness of the film and is 1.6 μOhm·m. For $L < 10$ with a decrease in the film thickness, the electrical resistivity increases sharply, reaching a value of about 3.2 μOhm·m for a film with $L = 3$ nm. The experimental results obtained are in good agreement with the data presented in the literature for β-Ta films of different thicknesses [34, 35].

According to structural studies, the average size of crystallites decreases significantly with the decreasing film thickness. A sharp increase in electrical resistance in the range of small thicknesses may be due to a decrease in the mean free path of metal conduction electrons due to a decrease in the size of the crystallites and an increase in the number of grain boundaries. An additional contribution to the resistance can be made by defects in the crystal lattice, the density of which is higher for metal films of small thickness in comparison with thicker films [36].

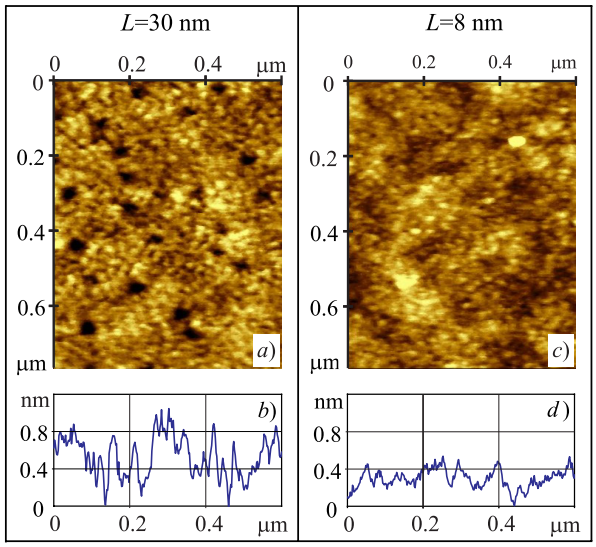


**Fig. 5.** Surface images (a, c) and surface profiles (b, d) of 30 and 8 nm thick Ta films

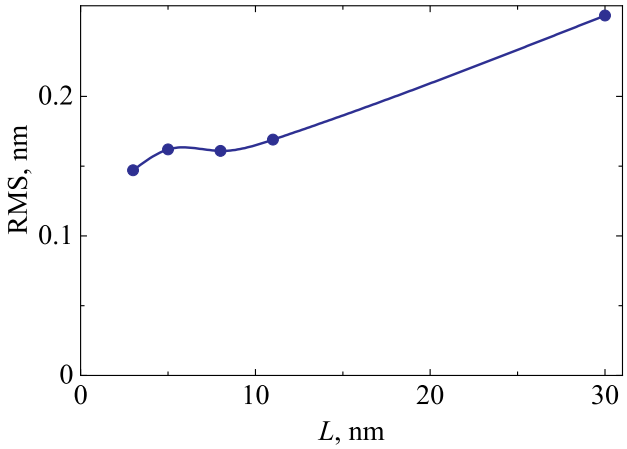


**Fig. 6.** Shows the dependence of the roughness parameter of the root mean square (RMS) on the thickness of the β-Ta film.

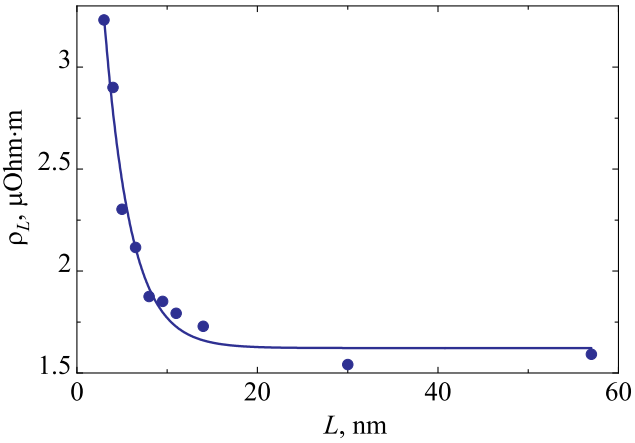


**Fig. 7.** Dependence of specific electrical resistivity of β-Ta $\rho_L$ films on the thickness at $T = 93$ K in the field $H = 0$. The experimental points are connected by a curve for ease of perception

The decrease in the size of the crystallites with a decrease in the film thickness is well consistent with the temperature coefficient of resistance (TCR) changes (Fig. 8).

For films in the thickness range of 3 ÷ 57 nm , a negative temperature coefficient of resistance was observed (see Fig. 8), characteristic of highly disordered systems [37, 38]. In this case, a decrease in temperature is accompanied by an increase in the specific electrical resistivity of the sample [39] (Fig. 8, insert).

An increase in the absolute value of TCR is observed with a decrease in film thickness and an increase in electrical resistance, which is associated with an increase in disorder in thinner layers of β-Ta. The charater of change in the dependence of TCR on $L$ is in good agreement with Moya's rule of thumb [38].

The field dependences of the electrical resistance of Ta films of different thicknesses were measured in a magnetic field applied in the plane of the film parallel and perpendicular to the direction of the current. The field varied from 20 to -20 and back to 20 kOe. The measurements were carried out at various fixed temperatures in the range from 93 to 343 K. Figure 9 shows the field dependences of the electrical resistivity $\rho_L(H)$ for a 5 nm thick Ta film.

With the collinearity of the current direction and the applied magnetic field ($\alpha = 0°$), the resistance increases with an increase in the applied field. If the field is perpendicular to the direction of the current ($\alpha = 90°$), then the changes in electrical resistance are within the measurement error. In our experiments, the non-zero longitudinal magnetoresistance was found for samples of Ta films with thicknesses from 3 to 11 nm. Similar field dependences of resistance were previously obtained for Pt [24-26] and β-Ta films [24].

Based on the results of measuring the field dependences of the resistivity of Ta films, the Hanle magnetoresistance (longitudinal magnetoresistance) $\mathcal{R}_L(H)$ was estimated. In our experiments, the maximum value of the applied magnetic field was 20 kOe, respectively, the maximum obtained value of the longitudinal magnetoresistance $\mathcal{R}_L(H = 20\ \text{kOe})$ was estimated for $|H| = 20$ kOe.

The field dependences of the longitudinal magnetoresistance of the β-Ta film with a thickness of 5 nm were measured at various fixed temperatures in the range 93 ÷ 343K. Figure 10 shows the temperature dependence of $\mathcal{R}_L(H = 20\ \text{kOe})$.

The maximum magnetoresistance of the film increases monotonously with the decreasing temperature. In a similar

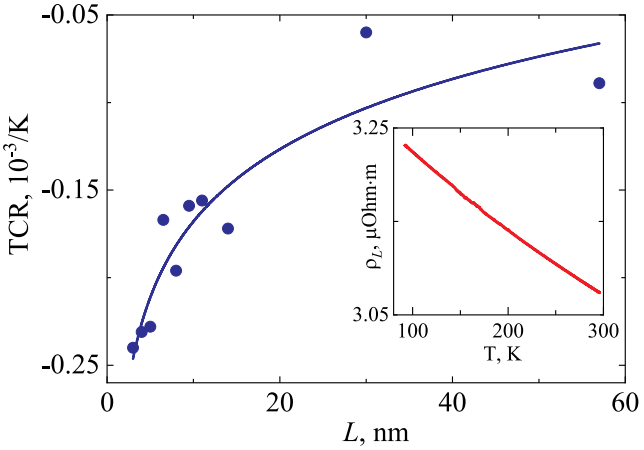


**Fig. 8.** The dependence of the temperature coefficient of resistance TCR on the thickness β-Ta in the field $H = 0$. On the insert the dependence $\rho_L(T)$ for a film is β-Ta with a thickness of 3 nm in the field $H = 0$. The experimental points are connected by a curve for the convenience of perceiving

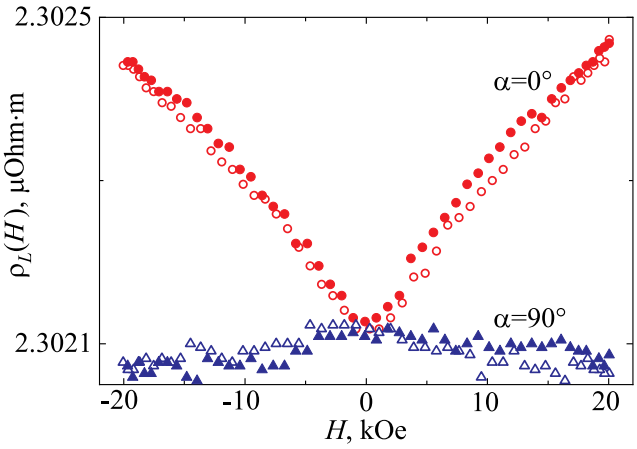


**Fig. 9.** Field dependences of the resistivity of the Ta film sample with a thickness of 5 nm at a temperature of 93 K. Solid circles and triangles measuring -20 to 20 kOe, unfilled circles and triangles measuring from 20 to -20 kOe

temperature range, similar dependences were observed for Pt films in the works [24, 25]. A possible explanation for the increase in longitudinal magnetoresistance with a decrease in temperature is an increase in the of the spin relaxation and, accordingly, an increase in the spin diffusion length.

The field dependences of the magnetoresistance of β-Ta films were measured at various fixed angles α in the range from -60° to 240°. Fig. 11 shows the angular dependences of $\mathcal{R}_L(H = 20\,\text{kOe}, \alpha)$ for Ta films with a thickness of 5 and 8 nm at $T = 103$K.

In both cases, the experimental points are close to the curve corresponding to the approximating function $\mathcal{R}_L(H = 20\,\text{kOe}, \alpha) \sim \cos^2\alpha$. With the perpendicular orientation of the current direction and the applied field ($\alpha = 90°$), magnetoresistance is not observed. The highest magnetoresistance $\mathcal{R}_L(H = 20\,\text{kOe})$ was obtained with collinear orientation of the current and field directions ($\alpha = 0$ and 180°).

Fig. 12 shows the dependence of $\mathcal{R}_L(H = 20\,\text{kOe})$ on the thickness of Ta films at a temperature of 93 K. The highest value of $\mathcal{R}_L(H = 20\,\text{kOe})$ was observed for β-Ta films with a thickness of 5 nm.

## 6. SPIN DIFFUSION LENGTH, SPIN RELAXATION TIME AND SPIN HALL ANGLE IN TANTALUM NANOLAYERS

We will analyze the experimental data obtained using the theory of dimensional effects in Hanle magnetoresistance presented in section 2.

To analyze the experimental dependences of the Hanle magnetoresistance, we use the expression (17). The surface scattering of electrons with a spin flip leads, firstly, to a decrease in the magnitude of the Hanle magnetoresistance and, secondly, to a change in the shape of the functional dependence of the magnetoresistance on the magnetic field. The decrease in the magnitude of the Hanle magnetoresistance is described by the first multiplier in the right part of the expression (17). The change in the shape of the magnetic resistance curve $\mathcal{R}_L(B)$ is described depending on the parameter ψ of the third factor enclosed in square brackets. As the numerical analysis of the expression (17) shows, the effect of surface scattering with a spin flip on the shape of the curve $\mathcal{R}_L(B)$ in the case of interest to us when $\varepsilon \le 1$, can be ignored.

Taking into account the above, the expression (17) can be written in the form

$$\mathcal{R}_L(B) \approx \xi_L^2 \frac{\text{th}\lambda}{\lambda}\left[1 - \text{Re}\frac{\text{th}\lambda\kappa}{\kappa\text{th}\lambda}\right], \qquad (20)$$

where $\xi_L$ is a parameter defined by the expression (19), expressed in terms of the spin Hall angle ξ and depending on the probability of surface scattering with a spin flip ε and the thickness of the film $L$. We will use formula (20) to describe experimentally observed dimensional effects in the Hanle magnetoresistance, considering $\xi_L$ to be a variable parameter whose value must be determined for each sample of a given thickness.

From the results of the section 5, shown in Fig. 7, it follows that in the absence of a magnetic field, the specific electrical resistivity

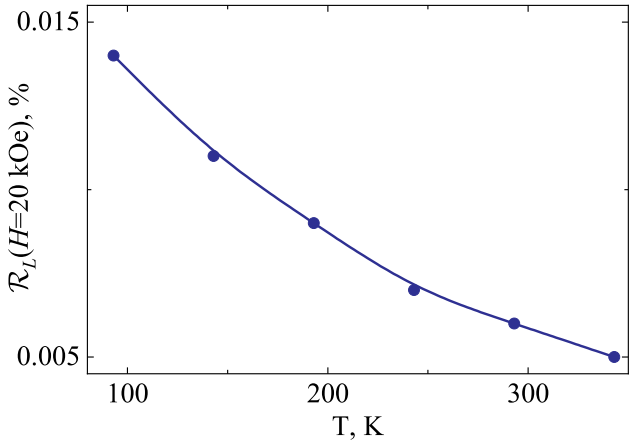


**Fig. 10.** Temperature dependence of longitudinal magnetoresistance for a β-tantalum film with a thickness of 5 nm. The experimental points are connected by a curve for ease of perception

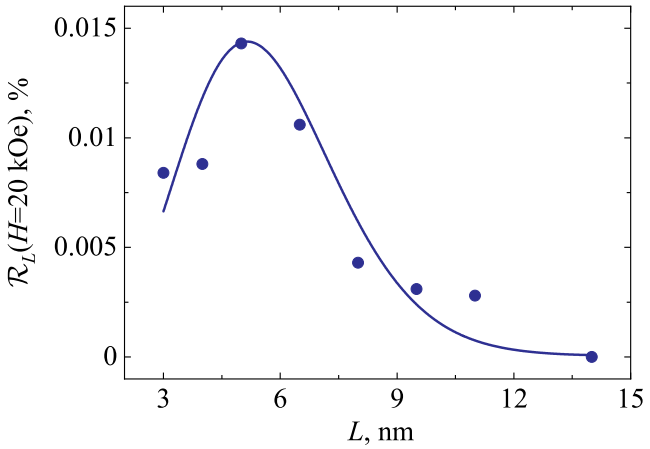


**Fig. 12.** Dependence of the Hanle magnetoresistance on the β-Ta film thickness at $T = 93$ K. The symbols correspond to the experimental values. The experimental points are connected by a curve for the convenience of perception

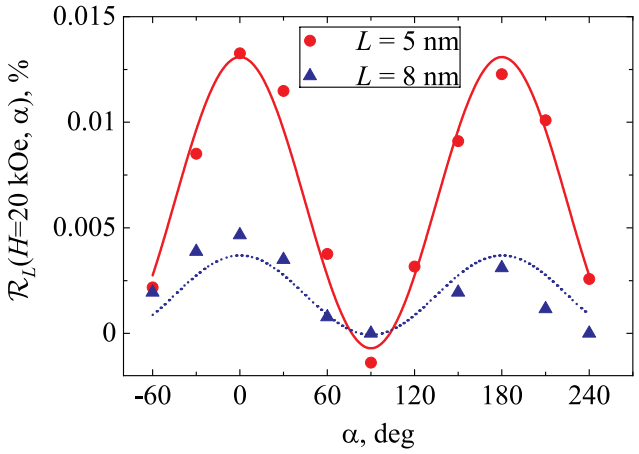


**Fig. 11.** Angular dependence of the magnetoresistance of β-tantalum films with thicknesses of 5 and 8 nm at $T = 103$ K. Circles and triangles are experimental points obtained for films with a thickness of 5 and 8 nm, respectively. Curves are the result is an approximation

$\rho_L$ of thin films of tantalum varies significantly with thickness. At $L > 30$ nm, electrical resistivity $\rho_L$ is practically independent of the film thickness, taking the value $\rho^{(bulk)} = 1.6$ μOhm·m, typical for massive β-Ta samples. For thicknesses $L < 10$ nm, electrical resistance $\rho_L$ increases significantly, reaching a value of about 3.2 μOhm·m for films with $L = 3$ nm. In fact, the value of the ratio $r_L = \rho_L / \rho^{(bulk)}$ can change twice.

The results of the investigation of the structure of β-Ta films presented in section 5 clearly indicate that the above-described behavior of $\rho_L$ correlates with a change in the microcrystalline structure of the films. According to structural studies, the average size of crystallites decreases significantly with a decrease in film thickness. A decrease in the size of the crystallites leads to an increase in the area of the intergranular boundaries and, as a result, to an increase in the relaxation rate of the pulse of conduction electrons $1 / \tau_O$ in the film. An additional contribution to the relaxation rate of $1 / \tau_O$ may be made by defects in the crystal lattice, the density of which is higher in films of metals of small thickness. Finally, the scattering of conduction electrons on the surface, which is responsible for the existence of the well-known classical dimensional effect in the electrical resistance of thin films, also makes a significant contribution to the dependence of $1 / \tau_O$ on $L$ [40].

It is natural to assume that the above-mentioned reasons for the possible dependence of the relaxation time of the pulse $\tau_O$ in the film on its thickness $L$ determine the experimentally observed dependence on the thickness of the relative electrical resistance $r_L = \rho_L / \rho^{(bulk)}$. Changes in electrical resistance caused by the accumulation of spin density near the boundaries of the sample, due to the smallness of the parameter $\xi^2 \ll 1$ make a small contribution to the dependence of the value of $\rho_L$ on $L$. Neglecting these small changes, we write down the relationship between the specific electrical resistivity of the film $\rho_L$ and the effective relaxation time of the pulse $\tau_O(L)$, depending on the thickness $L$, in the form $\rho_L = m_e / N_0 e^2 \tau_O(L)$. Writing down the specific electrical resistance of a massive metal as $\rho^{(bulk)} = m_e / N_0 e^2 \tau_O^{(bulk)}$, where $\tau_O^{(bulk)}$ is the pulse relaxation time in a solid metal, it is possible to put the dependence of $\tau_O(L)$ by the formula

$$\tau_O(L) = \tau_O^{(bulk)} / r_L. \qquad (21)$$

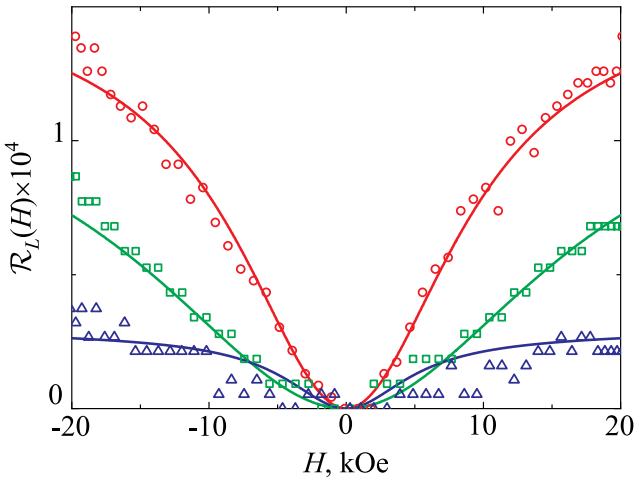


**Fig. 13.** Dependences of the Hanle magnetoresistance on the external magnetic field $H$ for β-tantalum films. The experimental data for films with a thickness of 3, 5 and 8 nm, respectively, are shown in square, round and triangular symbols. The green, red and blue solid lines correspond to the theoretical dependencies calculated by the formula (20)

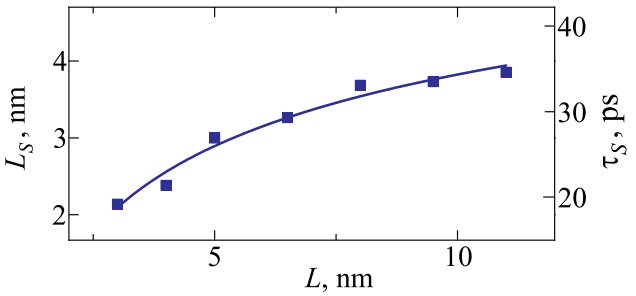


**Fig. 14.** Spin diffusion length $L_S$ (left scale) and spin relaxation time $\tau_S$ (right scale), determined from the analysis of experimental dependences of Hanle magnetoresistance for thin films is β-tantalum, as a function of the film thickness $L$. The points are connected by a curve for ease of perception

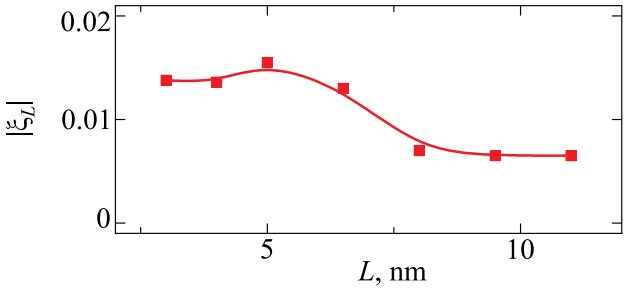


**Fig. 15.** The absolute value of the parameter $\xi_L$, determined from the analysis of experimental dependences of the Hanle magnetoresistance for thin β-tantalum films, as a function of the film thickness $L$. The points are connected by a curve for the convenience of perception

In this ratio, the value of $\tau_O^{(bulk)}$ is a parameter of the theory, whereas the value of $r_L$ is determined from the experiment.

Assuming that spin relaxation in tantalum films is due to a strong spin-orbit coupling, we will assume that the dependence on $L$ of the spin relaxation time $\tau_S(L)$ has the same form as the dependence (21) for $\tau_O(L)$:

$$\tau_S(L) = \tau_S^{(bulk)} / r_L. \qquad (22)$$

The value of $\tau_S^{(bulk)}$ appearing in (22) is a parameter of the theory, by analogy with $\tau_O^{(bulk)}$.

As a consequence, from the ratios (21) and (22), it is assumed that the length of the $L_S$ spin diffusion in the film will also depend on the thickness:

$$L_S(L) = L_S^{(bulk)} / r_L, \qquad (23)$$

where $L_S^{(bulk)}$ is the spin diffusion length in a massive metal.

Using expression (20), in which the dependences $\tau_S(L)$ and $L_S(L)$ are given by the relations (22) and (23), we have described the experimental dependences of the Hanle magnetoresistance $\mathcal{R}_L(H)$ on the external magnetic field $H$ for β-tantalum films of various thicknesses. The independent variable parameters were $\xi_L$, $\tau_S^{(bulk)}$ and $L_S^{(bulk)}$. Figure 13 shows the most typical experimental and theoretical results the dependence of the Hanle magnetoresistance on the external magnetic field for samples with thicknesses $L = 3$, 5 and 8 nm.

Experimental dependences of $\mathcal{R}_L(H)$ for the entire sample set ($L = 3$, 4, 5, 6.5, 8, 9.5, 11 nm) can be described at values $L_S^{(bulk)} = 4.34$ nm and $\tau_S^{(bulk)} = 3.9 \cdot 10^{-11}$ s. The values of the $L_S^{(bulk)}$ and $\tau_S^{(bulk)}$ pairs found are close to those obtained earlier by other research groups: the length of spin diffusion in tantalum $L_S \approx 2.7 \div 5.1$ nm [34, 41], the spin relaxation time in tantalum $\tau_S \approx 7.8 \cdot 10^{-12} \div 1.3 \cdot 10^{-11}$ s [42]. Fig. 14 shows the dependences of $\tau_S(L)$ and $L_S(L)$, constructed using the ratios (22) and (23), in which $L_S^{(bulk)} = 4.34$ nm and $\tau_S^{(bulk)} = 3.9 \cdot 10^{-11}$ s, and for $r_L$ the values are taken from the experiment.

Figure 14 shows that the spin diffusion length increases with the increasing thickness of the β- tantalum film. A similar trend in the spin diffusion length for a metal layer with a strong spin-orbit coupling was observed experimentally in [43].

Description of the entire set of experimental dependences of $\mathcal{R}_L(H)$ turned out to be possible only when taking into account the dependence of the parameter $\xi_L$ on the thickness of the film.

Figure 15 shows the found dependence of the absolute value of $\xi_L$ on the thickness of the film.

It follows from expression (19) that the condition $|\xi_L| \le |\xi|$ is satisfied for any value $L$. The values $|\xi_L|$ obtained by us allow us to find the minimum possible value $\xi^{(min)}$ of the absolute value of the spin Hall angle in β-tantalum: $\xi^{(min)} \approx 0.0155$. The value $\xi^{(min)}$ is the minimum value $|\xi|$, at which all our experimental data can be described consistently.

Let us analyze the dependence of the value of the parameter on the thickness of the film presented in Fig. 15 using the expression (19), according to which $\xi_L = \xi / \sqrt{1 + \psi \text{th}\lambda}$. Fig. 15 shows that $|\xi_L|$ varies in the range $0.0065 \div 0.0155$. The change in $|\xi_L|$ in this interval when the film thickness $L$ changes cannot be explained only on the basis of the explicit dependence of $\xi_L$ on the film thickness given in expression (19) by the $\text{th}\lambda$, function, since for the films under consideration its values weakly depend on $L$. Therefore, the change in $|\xi_L|$ in the interval under consideration can be described only if there is dependence of the probability of surface scattering with a spin reversal ε on $L$.

Note that using only the found values $|\xi_L|$, from expression (19) we cannot independently determine two parameters ξ and ε. In this regard, to determine the dependence of $\varepsilon(L)$ in our films, we use the value of ξ for tantalum, found experimentally in [44]. The authors of this work found that the spin Hall angle in β-tantalum is $\xi \approx -0.02$. Using this value of the spin Hall angle and taking the Fermi velocity equal to $v_F = 10^8$ cm/s (a close value was used in [8]), we obtained the dependence on the probability of surface scattering with a spin flip $\varepsilon(L)$, represented by in Fig. 16.

Fig. 16 shows the tendency of the increase of ε with the growth of the film thickness $L$. Such a characteristic dependence of $\varepsilon(L)$ correlates with the dependence of the square of surface roughness on the film thickness (see Fig. 6). It is difficult to expect a complete coincidence of these curves, since the probability of surface scattering with a spin flip depends not only on the RMS amplitude of the roughness, but also on their lateral size.

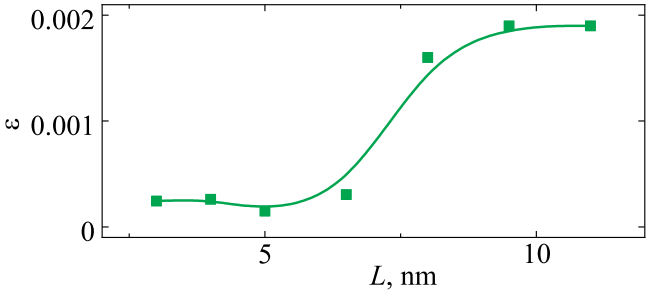


**Fig. 16.** Probability of surface scattering with spin flip ε as a function of film thickness $L$. The points are connected by a curve for ease of perception

Note that there are experimental papers in the literature [43, 45, 46] in which it was found that the spin Hall angle depends on the thickness of the film. In the light of the above results, it is impossible to exclude the possibility that conclusions about the dependence of the spin Hall angle on the film thickness were made without taking into account the influence of surface scattering with spin flip. In this paper, we demonstrate that in order to correctly extract data on the magnitude of the spin Hall angle, it is necessary to take into account surface scattering with a spin flip.

## 7. CONCLUSION

The paper presents a theory of dimensional effects in the magnetoresistance of thin films of normal metals arising from the presence of a strong spin-orbit coupling. The theory takes into account the scattering of conduction electrons with a spin flip on the film surfaces.

Within the framework of the constructed theory, it is shown that the spin-orbit coupling leads to an increase in the density of electric current near the boundaries of the film compared with the value of the current density in its depth. It is demonstrated that surface scattering with a spin flip, as well as an applied external magnetic field, leads to suppression of the accumulation of the spin moment of electrons near the film surfaces and thereby to a decrease in magnetoresistance.

Experimental studies of dimensional effects in magnetoresistance have been carried out on thin tantalum films obtained by magnetron sputtering. Studies of the microstructure have shown that mainly the β-phase is formed in tantalum films. As the film thickness increases, the crystallite size increases and the surface roughness increases.

According to the results of galvanomagnetic measurements, the studied β-tantalum films have a high electrical resistivity in the range of $1.6 \div 3.2$ μOhm ·m, as well as a negative temperature coefficient of electrical resistance.

The occurrence of positive longitudinal magnetoresistance in films has been detected in β-tantalum films in the thickness range of $3 \div 11$ nm. The experimental data are analyzed using the constructed theory. As a result, it was found that in the studied series of β-tantalum nanolayers, the spin diffusion length varies depending on the film thickness in the range $L_S \approx 2.14 \div 3.85$ nm, the spin relaxation time varies in the interval $\tau_S \approx 1.9 \cdot 10^{-11} \div 3.5 \cdot 10^{-11}$ s. In massive β-tantalum, the spin

diffusion length is $L_S^{(bulk)} = 4.34$ nm, and the spin relaxation time is $\tau_S^{(bulk)} = 3.9 \cdot 10^{-11}$s. The minimum value of the absolute value of the spin Hall angle at which our experimental data can be described is $\xi^{(min)} \approx 0.0155$. It is demonstrated that in order to correctly extract the spin Hall angle, it is necessary to take into account surface scattering with a spin flip. It is shown that the dependence of the probability of spin flip scattering on the film surfaces on its thickness correlates with the dependence of the square of the surface roughness on the film thickness.

## FUNDING

The work was carried out with financial support from the Russian Science Foundation within the framework of project No. 22-22-00220.

## REFERENCES

1. M. I. Dyakonov and V. I. Perel, JETP Letters **13**, 467 (1971)
2. M. I. Dyakonov and V. I. Perel, Phys. Lett. A **35**, 459 (1971).
3. J.-N. Chazalviel, Phys. Rev. B **11**, 3918 (1975).
4. J. E. Hirsch, Phys. Rev. Lett. **83**, 1834 (1999).
5. S. Zhang, Phys. Rev. Lett. **85**, 393 (2000).
6. A. Hoffmann, IEEE Trans. Magn. **49**, 5172 (2013).
7. Y. Niimi and Y. Otani, Rep. Prog. Phys. **78**, 124501 (2015).
8. J. Sinova, S. O. Valenzuela, J. Wunderlich, C. H. Back, and T. Jungwirth, Rev. Mod. Phys. **87**, 1213 (2015).
9. Spin Physics in Semiconductors, ed. by M. I. Dyakonov, Springer International Publishing, Cham (2017), p 532.
10. Y. K. Kato, R. C. Myers, A. C. Gossard, and D. D. Awschalom, Science **306**, 1910 (2004).
11. J. Wunderlich, B. Kaestner, J. Sinova, and T. Jungwirth, Phys. Rev. Lett. **94**, 047204 (2005).
12. S. O. Valenzuela and M. Tinkham, Nature **442**, 176 (2006).
13. T. Kimura, Y. Otani, T. Sato, S. Takahashi, and S. Maekawa, Phys. Rev. Lett. **98**, 156601 (2007).
14. T. Seki, Y. Hasegawa, S. Mitani, S. Takahashi, H. Imamura, S. Maekawa, J. Nitta, and K. Takanashi, Nat. Mater. **7**, 125 (2008).
15. Y. Niimi, H. Suzuki, Y. Kawanishi, Y. Omori, T. Valet, A. Fert, and Y. Otani, Phys. Rev. B **89**, 054401 (2014).
16. A. Manchon, J. Zelezny, I. M. Miron, T. Jungwirth, J. Sinova, A. Thiaville, K. Garello, and P. Gambardella, Rev. Mod. Phys. **91**, 035004 (2019).
17. Y. Cao, G. Xing, H. Lin, N. Zhang, H. Zheng, and K. Wang, iScience **23**, 101614 (2020).
18. K. Ando, Proc. Jpn. Acad., Ser. B **97**, 499 (2021).
19. D. Go, D. Jo, H.-W. Lee, M. Klaui, and Y. Mokrousov, Europhys. Lett. **135**, 37001 (2021).
20. R. Ramaswamy, J. M. Lee, K. Cai, and H. Yang, Appl. Phys. Rev. **5**, 031107 (2018).
21. A. Meo, C. E. Cronshaw, S. Jenkins, A. Lees, and R. F. L. Evans, J. Phys. Condens. Matter. **35**, 025801 (2023).
22. A. A. Stashkevich, J. of the Russian Universities. Radioelectronics **22**, 45 (2019).
23. M. I. Dyakonov, Phys. Rev. Lett. **99**, 126601 (2007).
24. S. Velez, V. N. Golovach, A. Bedoya-Pinto, M. Isasa, E. Sagasta, M. Abadia, C. Rogero, L. E. Hueso, F. S. Bergeret, and F. Casanova, Phys. Rev. Lett. **116**, 016603 (2016).
25. H. Wu, X. Zhang, C. H. Wan, B. S. Tao, L. Huang, W. J. Kong, and X. F. Han, Phys. Rev. B **94**, 174407 (2016).
26. J. Li, A. H. Comstock, D. Sun, and X. Xu, Phys. Rev. B **106**, 184420 (2022).
27. V.V. Ustinov, I. A. Yasyulevich, Physics of Metals and Metallography **121**, 223 (2020).
28. V.V. Ustinov and I. A. Yasyulevich, Phys. Rev. B **102**, 134431 (2020).
29. V. I. Okulov and V. V. Ustinov, Fiz. Met. Metaloved. **44**, 30 (1977).
30. V.V. Ustinov, Theor. Math. Phys. **44**, 814 (1980).
31. J. D. Zuo, Y. Q. Wang, K. Wu, J. Y. Zhang, G. Liu, and J. Sun, Scr. Mater. **212**, 114582 (2022).
32. M. Magnuson, G. Greczynski, F. Eriksson, L. Hultman, and H. Hogberg, Appl. Surf. Sci. **470**, 607 (2019).
33. E. A. I. Ellis, M. Chmielus, and S. P. Baker, Acta. Mater. **150**, 317 (2018).
34. R. Yu, B. F. Miao, L. Sun, Q. Liu, J. Du, P. Omelchenko, B. Heinrich, M. Wu, and H. F. Ding, Phys. Rev. Mater. **2**, 074406 (2018).
35. D. Qu, S. Y. Huang, B. F. Miao, S. X. Huang, and C. L. Chien, Phys. Rev. B **89**, 140407 (2014).
36. B. M. S. Bist and O. N. Srivastava, Thin Solid Films **18**, 71 (1973).
37. P. A. Lee and T. V. Ramakrishnan, Rev. Mod. Phys. **57**, 287 (1985).
38. J. H. Mooij, Phys. Status Solidi A **17**, 521 (1973).
39. N. Schwartz, W. A. Reed, P. Polash, and M. H. Read, Thin Solid Films **14**, 333 (1972).
40. M. A. Angadi, J. Mater. Sci. **20**, 761 (1985).
41. M. Morota, Y. Niimi, K. Ohnishi, D. H. Wei, T. Tanaka, H. Kontani, T. Kimura, and Y. Otani, Phys. Rev. B **83**, 174405 (2011).
42. C. Fang, C. H. Wan, B. S. Yang, J. Y. Qin, B. S. Tao, H. Wu, X. Zhang, X. F. Han, A. Hoffmann, X. M. Liu, and Z. M. Jin, Phys. Rev. B **96**, 134421 (2017).

43. Y. Saito, N. Tezuka, S. Ikeda, and T. Endoh, AIP Adv. **11**, 025007 (2021).
44. C. Hahn, G. de Loubens, O. Klein, M. Viret, V. V. Naletov, and J. Ben Youssef, Phys. Rev. B **87**, 174417 (2013).
45. Y. Wang, P. Deorani, X. Qiu, J. H. Kwon, and H. Yang, Appl. Phys. Lett. **105**, 152412 (2014).
46. J. T. Brangham, K.-Y. Meng, A. S. Yang, J. C. Gallagher, B. D. Esser, S. P. White, S. Yu, D. W. McComb, P. C. Hammel, and F. Yang, Phys. Rev. B **94**, 054418 (2016).